ORIGINAL PAPER

Journal of Anatomy ANATOMICAL SOCIETY WILEY

Nasal asymmetry changes during growth and development in 6- to 12-year-old children with repaired unilateral cleft lip and palate: A 3D computed tomography analysis

Le Huang[1,2] | Ziling Wang[3] | Zhiyi Shan[4] | Andy Wai Kan Yeung[5] | Yanqi Yang[4] | Zhigang Liang[2] | Min Gu[4] [ID]

[1]Department of Stomatology, Shenzhen Luohu Hospital Group Luohu People's Hospital, Guangdong, P.R. China

[2]Department of Stomatology, Shenzhen Second People's Hospital, Guangdong, P.R. China

[3]Faculty of Dentistry, The University of Hong Kong, Hong Kong S.A.R., China

[4]Orthodontics, Division of Paediatric Dentistry and Orthodontics, Faculty of Dentistry, The University of Hong Kong, Hong Kong S.A.R., China

[5]Applied Oral Sciences & Community Dental Care, Faculty of Dentistry, The University of Hong Kong, Hong Kong S.A.R., China

Correspondence
Zhigang Liang, Department of Stomatology, Second People Hospital of Shenzhen, Guangdong, P.R. China.
Email: liangzhigang@yeah.net

Min Gu, Orthodontics, 2/F, Prince Philip Dental Hospital, 34 Hospital Road, Sai Ying Pun, Hong Kong S.A.R., China
Email: drgumin@hku.hk

Funding information
The present study was supported by a grant of the Special Fund for High-Level Hospital Construction of Shenzhen Second People's Hospital (Ref. 4001018_2018).

Abstract

Repaired unilateral cleft lip and palate (UCLP) is often accompanied by the deformity and asymmetry of the nasal region. Three-dimensional analysis was performed to investigate the relationship between nasal soft- and hard-tissue asymmetries, as well as the changes in nasal asymmetry with age, among children with repaired UCLP (age: 6–12 years). Forty-seven patients were included in this study. Their computed tomography records were retrieved for analysis of the 3D asymmetry of 10 landmarks of the nasal soft and hard tissues. We observed that asymmetry was more severe in nasal hard tissues than in soft tissues, particularly in the sagittal dimension. Compared with patients aged 6–9 years old, patients aged 10 to 12 years old had significantly increased vertical asymmetry at the base of the alar groove (Gbase, $p = 0.027$) and the lateral point of the piriform aperture (LPA), ($p < 0.001$). The correlation between the LPA and the alar region was weak to moderate ($r = 0.290$ to 0.488). In conclusion, we found no evidence of growth and development in nasal hard-tissue asymmetry among 6- to 12-year-old children with repaired UCLP, except for the vertical dimension. Nasal soft tissue exhibited a more preferable symmetry than hard tissue, and this could be attributed to the compensatory growth of nasal soft tissue, particularly in the vertical and sagittal dimensions. The weak to moderate correlations between nasal soft-tissue asymmetry and hard-tissue asymmetry were observed in the three dimensions. Surgeons should consider these factors when repositioning the nasal alar and controlling the size of the nostrils.

KEYWORDS
3D analysis, nasal tissue asymmetry, repaired cleft lip and palate

---

1 | INTRODUCTION

Cleft-related nasal deformity is common among patients with repaired complete unilateral cleft lip and palate (UCLP) and severely affects the esthetics and psychology of patients (Mossey et al., 2009). This deformity could be due to both the primary deformity of the underlying hard tissues and a secondary deformity that mainly arises from iatrogenic factors and tissue scarring.

For primary hard-tissue deformity, the appearance of the soft tissue of the nose could reflect the underlying structure of the piriform aperture, nasal bones, and nasal cartilages because the nasal alar base adheres to the corresponding margin of the piriform aperture (Yang et al., 2016). Alveolar bone grafting can significantly improve nasal symmetry (Li et al., 2012; Zhang et al., 2014), although the bony depression and deformity of the piriform aperture do not necessarily cause nasal alar depression (Miyamoto et al., 2007). Additionally, alveolar bone grafting provides little support to the improvement of nasal symmetry (Rahpeyma & Khajehahmadi, 2015; Zhang et al., 2014).

Growth-related nasal deformity or secondary deformity due to environmental factors also accounts for an unfavorable soft-tissue appearance. In children, nasal deformity usually worsens with age. Sequential treatments are needed to restore esthetic appearance (Fisher et al., 2014). Ideal procedures and timings include primary rhinoplasty at the time of initial lip repair, intermediate rhinoplasty before school age, and secondary rhinoplasty after puberty (Kaufman et al., 2012). A one-stage primary correction of lip and nose deformities could adversely affect the growth of the nasal cartilage, thus resulting in worsened nasal deformity (Allori & Mulliken, 2017). Some researchers also recommended a 1 mm overcorrection of the nostril on the cleft side to the contralateral side during synchronous lip and nose repair to compensate for relapse and differential growth (Liou et al., 2004; Lo, 2006). However, a recent study indicated that the nostril width only expanded by 0.3 mm on average after surgery, thus indicating that overcorrection might not be necessary (Cutting, 2012).

Currently, it is still unclear whether nasal hard-tissue deformity can deteriorate nasal soft-tissue appearance in children with repaired UCLP and cause growth-related changes in nasal deformity. Thus, we investigated the relationship between asymmetries in the nasal soft tissue and hard tissue. Additionally, we examined the effects of growth and development on nasal appearance in children with repaired complete UCLP.

2 | METHODS

2.1 | Sample size calculation

According to a previous methodology (Wu et al., 2013), detecting an effect size of 1.136 for the horizontal difference in the distances from the lateral point of the piriform aperture to the facial midline requires a minimum sample size of 36 (18 in each group) at the 0.05% significance level by using G*Power (version 3.1.9.2, Kiel University; Faul et al., 2007) with a power of 90%.

2.2 | Inclusion criteria

Children (6 to 12 years old) with repaired UCLP who attended the Second Hospital of Shenzhen with maxillary computed tomography (CT) records available from January 2010 to August 2019 were included. Patients with a history of maxillofacial trauma, orthodontic treatment, alveolar bone grafting, and incomplete or blurry records were excluded. Eventually, 47 patients were enrolled, and their CT data were retrieved. All patients underwent a standard UCLP repair procedure, which included a simultaneous correction of the lip and nose and a routine ala nasi retraction in the first stage of surgery. Patients were divided into two groups by their age: 6- to 9-year-old group ($n = 24$; 15 males; average age $= 8.1 \pm 1.0$ years) and 10- to 12-year-old group ($n = 23$; 15 males; average age $= 10.6 \pm 0.8$ years).

This retrospective study was approved by the ethics committee of the Second Hospital of Shenzhen (No. 20200422012).

2.3 | CT scan

Spiral CT images (SOMATOM Definition AS, Siemens) were obtained from all patients before the alveolar bone grafting surgery. Scanning was performed in the head-first supine position and stationary state (no coughing or swallowing). The minimal field of view was the whole maxilla, and the slice thickness was 0.6 mm.

2.4 | Image processing and measurements

All raw CT records were saved in Digital Imaging and Communications in Medicine format and imported into Mimics software (v. 21.0; Materialize). The default thresholds for soft and hard tissues were −700 HU to 300 HU and 300 HU to 3071 HU respectively. After obtaining the soft- and hard-tissue masks, 3D model reconstruction was performed. The "Measure and Analyze" function under the "ANALYZE" bar was selected. The localization of landmarks for coordinates was verified in both the 3D multiplanar reconstruction window and the 3D model.

A Cartesian coordinate system was established by confirming the three reference planes in the hard-tissue model. The midsagittal plane was established using the sella (S), nasion (N), and basion (Ba). The transverse plane was established as the plane passing through the frontozygomatic point (FZ) and N perpendicular to the midsagittal plane. The coronal plane was established as the plane passing through the N perpendicular to the sagittal and horizontal planes. Three pairs of hard-tissue landmarks and four pairs of soft-tissue landmarks were located, including the inferior point of the nasomaxillary suture (INM), lateral point of the piriform aperture

TABLE 1 Reference planes, landmarks, and descriptions

| Planes and landmarks	Abbreviation	Description	From
Reference plane			
Sella	S	Center of the space in sella turcica	Green et al. (2017)
Nasion	N	Midpoint of the most anterior aspect of the frontonasal suture	Green et al. (2017)
Basion	Ba	Mid-dorsal point of the anterior margin of the foramen magnum on the basilar part of the occipital bone	Green et al. (2017)
Frontozygomatic suture	FZ	Most medial and anterior point of the frontozygomatic suture at the level of the lateral orbital rim	Nur et al. (2016)
Soft-tissue landmark			
Pronasale	Prn	Most protruded point of the apex of the nose	Bugaighis et al. (2014)
Subnasale	Sn	Midpoint of maximum concavity where the upper lip skin meets the columella base	Bugaighis et al. (2014)
Base of the alar groove	Gbase	Most inferior point of the alar groove	Nkenke et al. (2006)
Lateral point of the alar groove	Glat	Most lateral point of the alar groove	Nkenke et al. (2006)
Subalare	Sbal	Point at the inner lower limit of each alar base	Bugaighis et al. (2014)
Subnasale inner	Sni	Midpoint of the columella on each side at the bottom line where the thickness of the columella is measured	Bugaighis et al. (2014)
Hard-tissue landmark			
Inferior point of the nasomaxillary suture	INM	Most inferior point of the nasomaxillary suture	Moreddu et al. (2013)
Lateral point of the piriform aperture	LPA	Most lateral point of the piriform aperture	Moreddu et al. (2013)
Inferior point of the piriform aperture	IPA	Most inferior point of the piriform aperture	Moreddu et al. (2013)
Rhinion	Rh	Most anterior margin of the nasal bone	Inada et al. (2009)
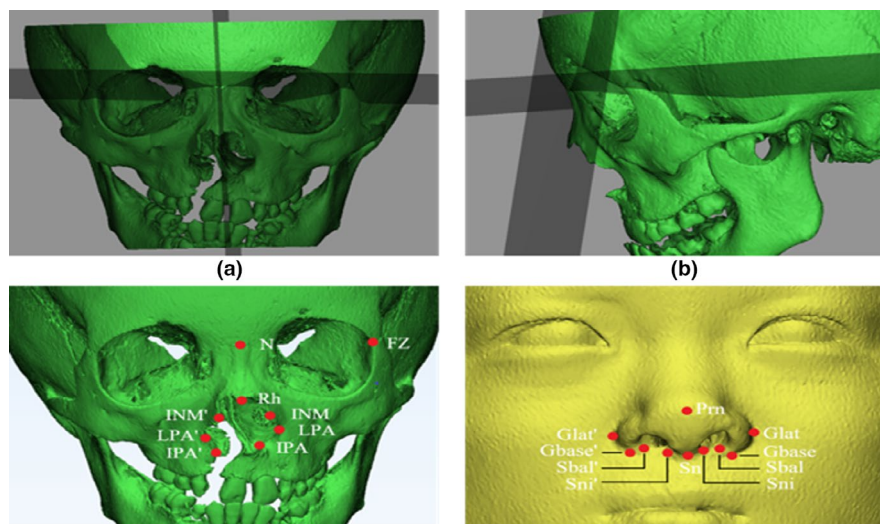
FIGURE 1 Reference planes and landmarks. (a and b) show the three reference planes (transverse, midsagittal, and coronal planes) used in the current study, (c and d) show the nasal hard- and soft-tissue landmarks used. FZ, frontozygomatic suture; Gbase, base of the alar groove; Glat, lateral point of the alar groove; INM, inferior point of the nasomaxillary suture; IPA, inferior point of the piriform aperture; LPA, lateral point of the piriform aperture; N, nasion; Prn, pronasale; Rh, rhinion; Sbal, subalare; Sn, subnasale; Sni, subnasale inner

(LPA), inferior point of the piriform aperture (IPA), base of the alar groove (Gbase), lateral point of the alar groove (Glat), subalare (Sbal), and subnasale inner (Sni; Table 1; Figure 1). The absolute distances were measured from each landmark to the midsagittal, transverse, and coronal reference planes as X, Y, and Z respectively. Asymmetry was quantified in the horizontal, vertical, and sagittal dimensions by calculating the difference in the absolute distances (X, Y, and Z) between the left and right landmarks to the

TABLE 2 Dahlberg errors

	X-coordinate		Y-coordinate		Z-coordinate	
Landmarks	Cleft side	Noncleft side	Cleft side	Noncleft side	Cleft side	Noncleft side
Prn	0.37					
Sn	0.57					
Gbase	0.93	0.8	0.73	0.49	1.13	1.18
Glat	0.68	0.73	0.71	0.52	1.04	1.15
Sbal	0.85	0.76	0.52	0.48	1.09	1.19
Sni	0.77	0.83	0.59	0.42	1.15	1.13
INM	0.77	0.71	0.52	0.75	0.85	0.95
LPA	0.40	0.43	1.05	0.85	1.09	1.05
IPA	0.91	1.17	1.54	1.29	1.46	1.41
Rh	0.29					

Abbreviations: Gbase, base of the alar groove; Glat, lateral point of the alar groove; INM, inferior point of nasomaxillary suture; IPA, inferior point of the piriform aperture; LPA, lateral point of the piriform aperture; Prn, pronasale; Rh, rhinion; Sbal, subalare; Sn, subnasale; Sni, subnasale inner.

corresponding reference plane. Two soft-tissue landmarks (pronasale [Prn] and subnasale [Sn]) and one hard-tissue landmark (rhinion [Rh]) at the midline were also registered and measured only for horizontal asymmetry (Figure 1).

2.5 | Statistical analysis

All measurements were performed by a single examiner (LH). Intraclass correlation (ICC) was evaluated by repeated measurements of 20 CT records that were randomly selected in a 2-week interval. Random error was calculated using the Dahlberg formula (Dahlberg, 1940): $ME = \sqrt{\Sigma d^2/2n}$, where d is the difference between the two measurements, and n is the sample size.

Normality of data was evaluated using the Shapiro–Wilk tests. Paired Student's t tests were used to compare the intragroup differences between the corresponding bilateral landmarks and midline landmarks to the midsagittal plane. Intergroup tests were performed using Student's two-sample t test. Pearson's tests were conducted to analyze the correlations between the asymmetries of the nasal soft tissues and hard tissues. All statistical analyses were performed using SPSS software (IBM Corp. Released 2013. IBM SPSS Statistics for Windows, version 22.0., IBM Corp.). Statistical significance was set at $p < 0.05$.

3 | RESULTS

3.1 | Method errors

Reliability tests revealed that all ICC values were between 0.83 and 0.99. Dahlberg random errors were between 0.29 and 1.54 mm (Table 2). Therefore, the measurement method was considered reliable.

3.2 | Nasal soft- and hard-tissue asymmetries in patients with repaired UCLP

Extensive 3D asymmetry was observed in the nasal tissue of 6- to 12-year-old patients with repaired UCLP, particularly for nasal hard-tissue landmarks (INM, IPA, LPA, and Rh) and soft-tissue landmarks at the midline (Prn and Sn; Table 3).

The severity of asymmetry in the nasal soft and hard tissues was similar in the horizontal dimension. More severe asymmetry in the nasal hard tissue was observed in the vertical and sagittal dimensions (Figure 2).

In the horizontal and sagittal dimensions, there were no significant differences between the two age groups for any landmark measurements (Tables 4 and 6, $p > 0.05$).

Significantly higher asymmetries in Gbase ($p < 0.05$) and LPA ($p < 0.001$) in the vertical dimension were detected in the 10- to 12-year-old group (1.60 and 2.65 mm, respectively) than in the 6- to 9-year-old group (0.93 and 1.35 mm, respectively; Table 5).

3.3 | Correlations between nasal soft- and hard-tissue asymmetries

In the horizontal and vertical dimensions, the asymmetries of soft- and hard-tissue landmarks for children (6–12 years old) with repaired UCLP were weakly to moderately correlated (0.00–0.19 very weak, 0.20–0.39 weak, and 0.40–0.59 moderate); the correlation coefficients ranged from −0.352 to 0.526 and from 0.293 to 0.488 respectively (Table 7). Notably, the midline landmark for hard tissue (Rh) was moderately correlated ($r = 0.417$) with that for soft tissue (Prn; $p < 0.01$). The correlation coefficients between the hard-tissue LPA and soft-tissue Gbase were 0.488 ($p < 0.01$) and 0.408 ($p < 0.01$) for LPA and soft-tissue Glat respectively.

In the sagittal dimension, soft- and hard-tissue landmarks were weakly correlated. There were no correlation coefficients >0.3 (Table 7).

TABLE 3 Horizontal discrepancies for midline landmarks from the midsagittal plane and comparison in the 3D distances from matched landmarks between the cleft and noncleft sides to the corresponding reference plane

Landmark	Axis	6- to 9-year-old group (N = 24)			10- to 12-year-old group (N = 23)		
		Cleft side Mean ± SD	Noncleft side Mean ± SD	p-value	Cleft side Mean ± SD	Noncleft side Mean ± SD	p-value
Soft tissue							
Prn	X	1.79 ± 0.92		<0.001***	1.54 ± 1.10		<0.001***
Sn	X	1.57 ± 0.76		<0.001***	1.59 ± 1.38		<0.001***
Gbase	X	14.84 ± 1.43	14.97 ± 1.89	0.627	16.60 ± 1.92	15.20 ± 2.37	0.039*
	Y	46.47 ± 3.60	46.61 ± 3.32	0.679	49.16 ± 4.08	49.93 ± 3.55	0.078
	Z	9.59 ± 5.84	9.06 ± 5.84	0.040*	9.52 ± 7.1	9.47 ± 7.06	0.412
Glat	X	17.68 ± 1.36	19.04 ± 1.83	0.022*	19.31 ± 1.94	19.39 ± 2.01	0.855
	Y	41.74 ± 3.70	41.04 ± 3.01	0.045*	44.09 ± 4.02	43.87 ± 2.92	0.690
	Z	9.23 ± 5.39	8.55 ± 5.40	0.030*	8.96 ± 6.46	9.37 ± 6.64	0.503
Sbal	X	10.20 ± 1.25	10.73 ± 1.99	0.331	11.38 ± 1.87	10.91 ± 2.06	0.361
	Y	45.59 ± 3.40	45.70 ± 3.26	0.898	48.43 ± 3.89	48.75 ± 3.19	0.543
	Z	8.74 ± 5.35	7.73 ± 5.21	0.002**	8.86 ± 6.53	7.87 ± 6.29	0.031*
Sni	X	2.40 ± 1.33	4.74 ± 1.33	0.001**	3.17 ± 1.54	4.60 ± 1.69	0.055
	Y	46.67 ± 3.18	46.48 ± 3.14	0.331	49.68 ± 3.30	49.65 ± 3.11	0.988
	Z	7.17 ± 4.98	6.67 ± 4.82	0.061	8.01 ± 5.89	7.02 ± 5.64	0.003**
Hard tissue							
INM	X	7.75 ± 1.10	9.20 ± 1.60	0.004**	8.23 ± 1.53	9.08 ± 1.24	0.066
	Y	29.05 ± 3.52	27.58 ± 3.46	<0.001***	31.11 ± 2.72	29.84 ± 2.47	0.004**
	Z	6.81 ± 3.70	5.21 ± 3.49	<0.001***	6.90 ± 4.61	5.57 ± 3.90	0.006**
LPA	X	12.00 ± 1.32	12.60 ± 1.64	0.219	13.50 ± 2.03	12.63 ± 1.57	0.136
	Y	34.87 ± 3.43	34.86 ± 2.86	0.954	37.38 ± 5.07	37.51 ± 3.28	0.704
	Z	15.99 ± 6.76	12.25 ± 5.67	<0.001***	18.51 ± 6.21	14.98 ± 5.74	<0.001***
IPA	X	9.47 ± 1.50	8.43 ± 2.15	0.175	10.99 ± 2.05	8.03 ± 1.79	0.004**
	Y	42.82 ± 4.65	39.66 ± 3.28	<0.001***	45.56 ± 5.63	43.09 ± 4.12	0.004**
	Z	20.52 ± 8.26	14.65 ± 6.57	<0.001***	21.74 ± 7.18	17.11 ± 6.29	<0.001***
sRh	X	1.01 ± 0.63		<0.001***	0.97 ± 0.74		<0.001***

Note: Unit: mm.

Abbreviations: Axis: X represents the distance from the landmarks to the midsagittal plane, Y represents the distance from the landmarks to the transverse plane, and Z represents the distance from the landmarks to the coronal plane; Gbase, base of the alar groove; Glat, lateral point of the alar groove; INM, inferior point of nasomaxillary suture; LPA, lateral point of the piriform aperture; Prn, pronasale; Rh, rhinion; Sbal, subalare; SD, standard deviation; Sn, subnasale.
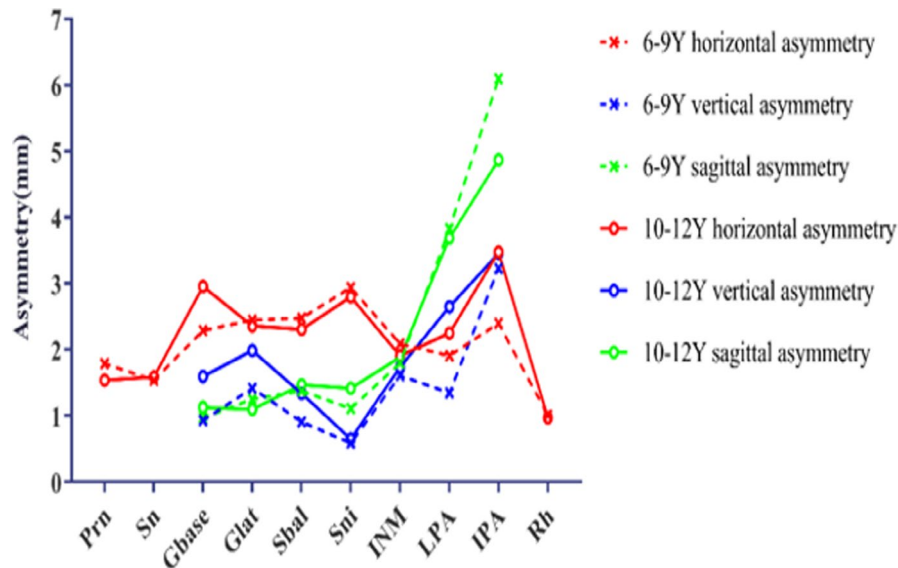
*p < 0.05; **p < 0.01; ***p < 0.001.

FIGURE 2 Descriptive results of the nasal 3D asymmetry. The red, blue, and green lines represent the nasal tissue landmark asymmetry in the horizontal, vertical, and sagittal dimensions respectively. The dotted and solid lines represent the 6- to 9-year-old patients and 10- to 12-year-old patients respectively. Gbase, base of the alar groove; Glat, lateral point of the alar groove; INM, inferior point of the nasomaxillary suture; IPA, inferior point of the piriform aperture; LPA, lateral point of the piriform aperture; Prn, pronasale; Rh, rhinion; Sbal, subalare; Sn, subnasale; Sni, subnasale inner

4 | DISCUSSION

4.1 | Selection of landmarks

In CT scans, the ideal landmarks are the margins, holes, apices of anatomical structures, or other structures that can be easily identified and located in 3D images, clearly observed in 3D structures, and verified in 2D-view windows (Wu et al., 2013). However, in patients with UCLP, the piriform aperture region presents with obvious bony defects, thereby reducing the number of reliable bony landmarks. The current study adopted landmarks that were mostly located at the junction of the anatomical structures (N, FZ, and INM), as previously established (Moreddu et al., 2013; Wu et al., 2013); the margin of the foramina (Ba, LPA, IPA, and Rh); and the turning point of the 3D structures (Gbase, Glat, Sbal, Sni, Prn, Sn; Bugaighis et al., 2014; Green et al., 2017; Inada et al., 2009; Lee et al., 2014; Moreddu et al., 2013; Nkenke et al., 2006; Nur et al., 2016; Yang et al., 2016) so that such landmarks could be accurately located in the soft- and hard-tissue windows.

4.2 | Selection of reference planes

This study involved three midline landmarks (S, N, and Ba) to establish the midsagittal plane because this method has fewer variable factors and provides better accuracy for the analysis of facial symmetry (Patel et al., 2018). Green et al. (2017) evaluated the accuracy of several midsagittal planes established by seven midline landmarks, including the S, N, Ba, crista galli, posterior nasal spine, anterior nasal spine, and incisive foramen (IF). The plane located by

the N, Ba, and IF had the best accuracy, whereas the plane established with S, N, and Ba had preferable accuracy. For patients with UCLP, the IF showed more positional variations and poorer sharpness for localization because of the cleft compared with the landmarks on the base of the skull that are relatively stable (Kyrkanides et al., 2000). The current study used the S, N, and Ba to establish the midsagittal plane.

4.3 | Method errors

The Dahlberg method error indicated slightly more evident method errors in IPA than other landmarks: the highest was 1.54 mm. This is because the IPA is the margin of the cleft, and the bone deficit resulted in a hardly defined IPA. Given that the corresponding distances from the cleft-side IPA to the transverse plane were 42.82 and 45.56 for the 6- to 9-year-age group and 10- to 12-year-age group, respectively, this error constitutes an approximately 3%–4% difference that in itself may have no clinical significance. In addition, the sagittal plane was last defined by the horizontal and vertical planes; therefore, the method errors in the sagittal dimension were also notable compared with other dimensions. However, an error of approximately 1 mm should not appreciably affect the results of our study.

4.4 | Growth and development of nasal horizontal asymmetry

No significant change in asymmetry during growth and development was observed in the horizontal dimension between the 6- to 9-year-old

TABLE 4 Nasal asymmetry changes in the horizontal dimension

	6- to 9-year-old group (N = 24)				10- to 12-year-old group (N = 23)					
			95% CI				95% CI			
Landmark	Mean	SD	Lower	Upper	Mean	SD	Lower	Upper	Diff	p-value
Soft tissue										
Prn	1.79	0.92	1.40	2.18	1.54	1.10	1.06	2.02	−0.25	0.395
Sn	1.54	0.76	1.22	1.86	1.59	1.38	1.00	2.19	0.05	0.878
Gbase	2.29	1.60	1.62	2.96	2.96	1.66	2.24	3.68	0.67	0.164
Glat	2.45	1.55	1.80	3.11	2.36	1.16	1.86	2.87	−0.09	0.829
Sbal	2.48	1.41	1.88	3.07	2.31	1.33	1.73	2.88	−0.17	0.675
Sni	2.94	1.66	2.24	3.64	2.80	1.86	2.00	3.61	−0.14	0.790
Hard tissue										
INM	2.09	1.36	1.51	2.66	1.91	1.28	1.36	2.47	−0.18	0.649
LPA	1.91	1.21	1.40	2.42	2.25	1.45	1.63	2.88	0.34	0.382
IPA	2.40	2.00	1.56	3.25	3.48	2.23	2.52	4.45	1.08	0.087
Rh	1.01	0.63	0.75	1.28	0.97	0.74	0.65	1.29	−0.04	0.822

Note: Unit: mm.

Abbreviations: CI, confidence interval; Diff, mean difference; Gbase, base of the alar groove; Glat, lateral point of the alar groove; INM, inferior point of the nasomaxillary suture; IPA, inferior point of the piriform aperture; LPA, lateral point of the piriform aperture; Prn, pronasale; Rh, rhinion; Sbal, subalare; SD, standard deviation; Sn, subnasale; Sni, subnasale inner.

TABLE 5 Nasal asymmetry changes in the vertical dimension

	6- to 9-year-old group (N = 24)				10- to 12-year-old group (N = 23)					
			95% CI				95% CI			
Landmark	Mean	SD	Lower	Upper	Mean	SD	Lower	Upper	Diff	p-value
Soft tissue										
Gbase	0.93	0.82	0.58	1.27	1.60	1.16	1.10	2.10	0.67	0.027[*]
Glat	1.42	0.98	1.00	1.83	1.99	1.25	1.45	2.53	0.57	0.085
Sbal	0.91	0.74	0.60	1.23	1.34	0.95	0.93	1.75	0.43	0.092
Sni	0.59	0.48	0.39	0.80	0.65	0.58	0.40	0.90	0.06	0.731
Hard tissue										
INM	1.61	1.26	1.08	2.14	1.74	1.56	1.07	2.42	0.13	0.748
LPA	1.35	0.89	0.97	1.72	2.65	1.16	2.14	3.15	1.30	< 0.001[***]
IPA	3.23	1.89	2.43	4.03	3.46	2.25	2.49	4.43	0.23	0.706

Note: Unit: mm.

Abbreviations: CI, confidence interval; Diff, mean difference; Gbase, base of the alar groove; Glat, lateral point of the alar groove; INM, inferior point of the nasomaxillary suture; IPA, inferior point of the piriform aperture; LPA, lateral point of the piriform aperture; Sbal, subalare; SD, standard deviation; Sni, subnasale inner.

[*]*p* < 0.05; [***]*p* < 0.001.

group and the 10- to 12-year-old group. This finding may be due to the fact that the width of the maxilla displayed the least change after birth, and the intermaxillary suture fused at age three to five years old (Manlove et al., 2020). Hence, the low potential of horizontal hard-tissue growth after school age did not result in changes to the asymmetry of the nasal hard tissue.

In theory, soft tissue has complementary growth that can partly compensate for hard-tissue deformities. However, a previous study indicated that the growth potential of nasal soft tissue in the horizontal dimension was limited after one year of age (Farkas et al., 1992). The current study also revealed that nasal soft tissue had only limited growth potential in the horizontal dimension in 6- to 12-year-olds.

Another point worth noting is that the midline landmarks had less asymmetry than the bilateral landmarks. This could be related to the direction of the maxillary growth. The maxilla presented with the least

TABLE 6 Nasal asymmetry changes in the sagittal dimension

| Landmark | 6- to 9-year-old group (N = 24) | | | | 10- to 12-year-old group (N = 23) | | | | Diff | p-value |
| | Mean | SD | 95% CI | | Mean | SD | 95% CI | | | |
			Lower	Upper			Lower	Upper		
Soft tissue										
Gbase	0.97	0.94	0.58	1.37	1.13	0.95	0.72	1.54	0.16	0.576
Glat	1.25	1.06	0.80	1.70	1.10	1.17	0.60	1.61	−0.15	0.654
Sbal	1.38	0.85	1.02	1.74	1.47	1.30	0.91	2.04	0.09	0.767
Sni	1.11	0.69	0.82	1.40	1.42	0.80	1.08	1.77	0.31	0.162
Hard tissue										
INM	1.80	1.25	1.27	2.33	1.89	1.33	1.31	2.46	0.09	0.825
LPA	3.83	1.89	3.03	4.63	3.69	2.25	2.71	4.66	−0.14	0.813
IPA	6.10	2.59	5.01	7.19	4.87	2.65	3.72	6.02	−1.23	0.115

Note: Unit: mm.

Abbreviations: CI, confidence interval; Diff, mean difference; Gbase, base of the alar groove; Glat, lateral point of the alar groove; INM, inferior point of the nasomaxillary suture; IPA, inferior point of the piriform aperture; LPA, lateral point of the piriform aperture; Sbal, subalare; SD, standard deviation; Sni, subnasale inner.

TABLE 7 Correlations between nasal soft- and hard-tissue asymmetries in the three dimensions

| | | | Hard tissue | | | | | | |
| | | | INM | | LPA | | | IPA | Rh |
			X	Z	X	Y	Z	X	X
Soft tissue	Prn	Coefficient	0.341				0.417		
		p-value	0.019*				0.004**		
	Sn	Coefficient	0.401						
		p-value	0.005**						
	Gbase	Coefficient		0.293	0.404	0.488		0.355	
		p-value		0.046*	0.005**	0.001**		0.014*	
	Glat	Coefficient	0.474		0.371	0.408			0.413
		p-value	0.001**		0.010*	0.004**			0.004**
	Sbal	Coefficient			0.345	0.293		−0.352	
		p-value			0.018*	0.046*		0.015*	
	Sni	Coefficient	0.526			0.290			
		p-value	<0.001***		0.048*				

Note: X represents the horizontal dimension, Y represents the vertical dimension, and Z represents the sagittal dimension.

Abbreviations: Gbase, base of the alar groove; Glat, lateral point of the alar groove; INM, inferior point of the nasomaxillary suture; IPA, inferior point of the piriform aperture; LPA, lateral point of the piriform aperture; Prn, pronasale; Rh, rhinion; Sbal, subalare; Sn, subnasale; Sni, subnasale inner.
*p < 0.05; **p < 0.01; ***p < 0.001.

changes in width after birth and grew forward and downward (Curti et al., 2019; Manlove et al., 2020). Additionally, the maxillary growth was centrifugal with limited movement in the central parts, such as the nose tip (Curti et al., 2019; Delaire, 1997). Moreover, the correction of the abnormal attachment of muscles during the first phase of nasolabial surgery also improved the midline symmetry of the nasal soft and hard tissues. Therefore, the asymmetry of the soft and hard tissues of the nasal midline is limited.

4.5 | Growth and development of nasal vertical asymmetry

The findings revealed that the asymmetry of the soft and hard tissues in the vertical dimension in the 6- to 9-year-old group was less than that in other dimensions, but it increased in the 10- to 12-year-old group. This finding may be due to the fact that most postnatal changes occur in the height of the maxilla (Proffit et al.,

2013), and the clockwise growth increases the height of the anterior maxilla (Doğan et al., 2006; Sasaki et al., 2004). This development pattern may worsen the inherent vertical deformity and asymmetry of the nasal hard tissue.

Lateral point of the piriform aperture and Gbase showed statistically significant changes probably because most maxillary growth changes occurred in the vertical dimension. However, abnormal muscular attachment, and imbalanced muscular tension on the skin, and scarring tissues could cause downward movements of the outer margin of the piriform aperture and the alar base owing to the lack of bony support under the alar base, thus deteriorating nasal vertical asymmetry.

It is worth noting that the change in LPA was less than the change in Gbase probably because the growth change in the nasal soft tissue was related to the underlying hard-tissue change but with greater growth potential to compensate for the underdevelopment of the hard tissue (Rahpeyma & Khajehahmadi, 2015). With such a compensatory capacity, the nasal soft tissue presented with less asymmetry in the vertical dimension. Li et al. (2012) also demonstrated that soft tissue at the nasal base could grow compensatively, thus raising the level of the nasal floor at the cleft side to the same level as the noncleft side and significantly reducing the vertical asymmetry of the nasal soft tissue.

4.6 | Growth and development of nasal sagittal asymmetry

This study demonstrated that the most severe asymmetry of the nasal hard tissue occurred in the sagittal dimension, but the asymmetry of the soft tissue was much less than the hard tissue. With growth and development, no significant changes were observed in the nasal soft- and hard-tissue asymmetries. This could be attributed to the progressive maxillary retrognathism and compensatory growth of the nasal soft tissue (Moreira et al., 2014). The absence of significant changes in nasal soft- and hard-tissue asymmetries with growth and development in the sagittal dimension was probably due to block movement rather than the differential dynamic deposition pattern of the maxilla before the age of 11–12 years (Delaire, 1997).

4.7 | Correlations between nasal soft- and hard-tissue asymmetries

The correlation between the landmark asymmetries of nasal soft tissues and hard tissues in patients with repaired UCLP was moderate in the horizontal and vertical dimensions. The INM and Sni were horizontally correlated ($r = 0.526$); no correlation was >0.6 probably because the asymmetry of the nasal bone could affect the position of the nasal septum to some extent, thus causing horizontal Sni asymmetry.

Similar to a previous study indicating that a weak correlation exists between nasal soft and hard tissues in patients with repaired UCLP (Urbanova et al., 2013), the current study revealed that statistically significant correlations exist between the asymmetries of

hard-tissue landmarks (LPA) and those for soft tissues (Gbase, Glat, and Sbal) in all three dimensions. This finding suggests that the restoration of the LPA is crucial for nasal alar symmetry. In addition, given that nasal ala symmetry could be concurrently affected by nasal cartilages, muscles, skin, subcutaneous tissues, mucosa, and scarring (Nakamura et al., 2010), the correction of cartilaginous deformity, relaxation of abnormally attached muscle, and prevention of scarring as much as possible are also vital to a prospective nasal alar symmetry.

4.8 | Clinical implications of the current study

Our results indicate that for 6- to 12-year-old patients with repaired UCLP, the horizontal growth potential and compensatory ability of nasal soft and hard tissues are limited. Therefore, the growth difference between cleft and noncleft sides is small; surgeons might not need to take the differential growth change into consideration in the correction of nasal secondary deformity in preschoolers. The usual protocol of a 1 mm compensatory retraction of the alar is not always necessary. The location for the repositioning of the nostrils and the size of the nostril should be the same as that on the noncleft side.

The worsening of the vertical asymmetry of the alar base could also indicate that the first stage of nasolabial surgery has not completely detached the abnormally attached muscles in the alar region or that postoperative care was inadequate and led to subsequent scar formation. Additionally, owing to the great growth potential in the vertical dimension, these factors could result in the displacement of the alar base during development because they exert abnormal tension. Therefore, the correction of abnormally attached muscle fibers in the alar region, particularly the vertical muscles, is crucial for restoring nose symmetry.

Alternatively, although soft tissue exhibited marked compensatory ability in the sagittal dimension, it could not completely compensate for sagittal hard-tissue deformity in the nasal region. Therefore, sagittal nasal asymmetry in most patients is likely to occur because of significant hard-tissue deformity and insufficient soft-tissue compensation. This suggests that most patients probably require alveolar bone grafting to restore the bony structures at the nasal base, particularly the bony depression at the outer margin of the piriform aperture. Furthermore, our results demonstrate that the lateral margin of the piriform aperture has a moderate correlation with some soft-tissue landmarks, including the Gbase, Glat, and Sbal. Hence, we believe that the restoration of the symmetry of the LPA via alveolar bone grafting might be necessary to acquire preferable nasal alar symmetry in patients with repaired UCLP.

4.9 | Limitations of the current study

We used CT to reconstruct a 3D mask of soft tissue. Mild errors may occur during the reconstruction procedure because of the absence

of a definite threshold for soft tissues and the relatively low imaging quality of CT compared with that of laser surface scanning or stereophotogrammetry. Moreover, given the limited number of adolescent and adult patients, these findings are limited in scope regarding the full picture of growth and development effects on children with repaired UCLP. Patients aged 6 to 12 years old, especially males, may not have reached peak growth; therefore, slight deviations may be present in the results. In the future, studies should be conducted with patients of a wider age range or with a longer term observation period to explore the growth and development of nasal soft- and hard-tissue asymmetries in patients with repaired UCLP and alveolar bone grafting.

5 | CONCLUSIONS

Except for the vertical dimension, we found no evidence of growth and development in the nasal hard-tissue asymmetry among 6- to 12-year-old children with repaired UCLP. Nasal soft tissue exhibited more preferable symmetry than hard tissue, which could be attributed to the compensatory growth in nasal soft tissue, particularly in the vertical and sagittal dimensions. By contrast, compensatory capacity was limited in the horizontal dimension. There were weak to moderate correlations between nasal soft- and hard-tissue asymmetries in the three dimensions. Surgeons should consider these factors when repositioning the nasal alar and controlling the size of the nostrils.

AUTHOR CONTRIBUTIONS

MG and ZGL conceived and designed the study. LH collected and analyzed the data and drafted the manuscript. ZLW, ZYS, AWKY, and YQY critically revised the manuscript. All authors read and approved the final version of the manuscript.

ORCID

Min Gu https://orcid.org/0000-0001-6447-9573

REFERENCES

Allori, A.C. & Mulliken, J.B. (2017) Evidence-based medicine: secondary correction of cleft lip nasal deformity. _Plastic and Reconstructive Surgery_, 140, 166e–176e.

Bugaighis, I., Mattick, C.R., Tiddeman, B. & Hobson, R. (2014) 3D asymmetry of operated children with oral clefts. _Orthodontics and Craniofacial Research_, 17, 27–37.

Curti, S.M., Barla, N., Bianchi, F.A., Di Vella, G., Orto, D., Ramieri, G.A. et al. (2019) Juvenile facial growth and mimicry: a preliminary 3D study. _Journal of Forensic Sciences_, 64, 1812–1816.

Cutting, C. (2012) Discussion. Fourth-dimensional changes in nasolabial dimensions following rotation-advancement repair of unilateral cleft lip. _Plastic and Reconstructive Surgery_, 129, 499–501.

Dahlberg, G. (1940) Statistical methods for medical and biological students. _Public Health_, 54, 92–93.

Delaire, J. (1997) Maxillary development revisited: relevance to the orthopaedic treatment of Class III malocclusions. _European Journal of Orthodontics_, 19, 289–311.

Doğan, S., Onçağ, G. & Akin, Y. (2006) Craniofacial development in children with unilateral cleft lip and palate. _British Journal of Oral and Maxillofacial Surgery_, 44, 28–33.

Farkas, L.G., Posnick, J.C., Hreczko, T.M. & Pron, G.E. (1992) Growth patterns of the nasolabial region: a morphometric study. _The Cleft Palate-Craniofacial Journal_, 29, 318–324.

Faul, F., Erdfelder, E., Lang, A.G. & Buchner, A. (2007) G*Power 3: a flexible statistical power analysis program for the social, behavioral, and biomedical sciences. _Behavior Research Methods_, 39, 175–191.

Fisher, M.D., Fisher, D.M. & Marcus, J.R. (2014) Correction of the cleft nasal deformity: from infancy to maturity. _Clinics in Plastic Surgery_, 41, 283–299.

Green, M.N., Bloom, J.M. & Kulbersh, R. (2017) A simple and accurate craniofacial midsagittal plane definition. _American Journal of Orthodontics and Dentofacial Orthopedics_, 152, 355–363.

Inada, E., Saitoh, I., Hayasaki, H., Iwase, Y., Kubota, N., Tokemoto, Y. et al. (2009) Relationship of nasal and skeletal landmarks in lateral cephalograms of preschool children. _Forensic Science International_, 191, 111.e1–111.e4.

Kaufman, Y., Buchanan, E.P., Wolfswinkel, E.M., Weathers, W.M. & Stal, S. (2012) Cleft nasal deformity and rhinoplasty. _Seminars in Plastic Surgery_, 26, 184–190.

Kyrkanides, S., Klambani, M. & Subtelny, J.D. (2000) Cranial base and facial skeleton asymmetries in individuals with unilateral cleft lip and palate. _The Cleft Palate-Craniofacial Journal_, 37, 556–561.

Lee, K.M., Lee, W.J., Cho, J.H. & Hwang, H.S. (2014) Three-dimensional prediction of the nose for facial reconstruction using cone-beam computed tomography. _Forensic Science International_, 236, 194.e1–194.e5.

Li, J., Shi, B., Liu, K. & Zheng, Q. (2012) A preliminary study on the hard-soft tissue relationships among unoperated secondary unilateral cleft nose deformities. _Oral Surgery, Oral Medicine, Oral Pathology and Oral Radiology_, 113, 300–307.

Liou, E.J., Subramanian, M., Chen, P.K. & Huang, C.S. (2004) The progressive changes of nasal symmetry and growth after nasoalveolar molding: a three-year follow-up study. _Plastic and Reconstructive Surgery_, 114, 858–864.

Lo, L.J. (2006) Primary correction of the unilateral cleft lip nasal deformity: achieving the excellence. _Chang Gung Medical Journal_, 29, 262–267.

Manlove, A.E., Romeo, G. & Venugopalan, S.R. (2020) Craniofacial growth: current theories and influence on management. _Oral and Maxillofacial Surgery Clinics of North America_, 32, 167–175.

Miyamoto, J., Nagasao, T., Nakajima, T. & Ogata, H. (2007) Evaluation of cleft lip bony depression of piriform margin and nasal deformity with cone beam computed tomography: "retruded-like" appearance and anteroposterior position of the alar base. _Plastic and Reconstructive Surgery_, 120, 1612–1620.

Moreddu, E., Puymerail, L., Michel, J., Achache, M., Dessi, P. & Adalian, P. (2013) Morphometric measurements and sexual dimorphism of the piriform aperture in adults. _Surgical and Radiologic Anatomy_, 35, 917–924.

Moreira, I., Suri, S., Ross, B., Tompson, B., Fisher, D. & Lou, W. (2014) Soft-tissue profile growth in patients with repaired complete unilateral cleft lip and palate: a cephalometric comparison with normal controls at ages 7, 11, and 18 years. _American Journal of Orthodontics and Dentofacial Orthopedics_, 145, 341–358.

Mossey, P.A., Little, J., Munger, R.G., Dixon, M.J. & Shaw, W.C. (2009) Cleft lip and palate. _The Lancet_, 374, 1773–1785.

Nakamura, N., Okawachi, T., Nishihara, K., Hirahara, N. & Nozoe, E. (2010) Surgical technique for secondary correction of unilateral cleft lip-nose deformity: clinical and 3-dimensional observations of preoperative and postoperative nasal forms. *Journal of Oral and Maxillofacial Surgery*, 68, 2248–2257.

Nkenke, E., Lehner, B., Kramer, M., Haeusler, G., Benz, S., Schuster, M. et al. (2006) Determination of facial symmetry in unilateral cleft lip and palate patients from three-dimensional data: technical report and assessment of measurement errors. *The Cleft Palate-Craniofacial Journal*, 43, 129–137.

Nur, R.B., Çakan, D.G. & Arun, T. (2016) Evaluation of facial hard and soft tissue asymmetry using cone-beam computed tomography. *American Journal of Orthodontics and Dentofacial Orthopedics*, 149, 225–237.

Patel, D.S., Jacobson, R., Duan, Y., Zhao, L., Morris, D. & Cohen, M.N. (2018) Cleft skeletal asymmetry: asymmetry index, classification and application. *The Cleft Palate-Craniofacial Journal*, 55, 348–355.

Proffit, W.R., Fields, H.W. & Sarver, D.M. (2013) *Contemporary orthodontics*, 5th edition. St. Louis, Mo.: Elsevier/Mosby.

Rahpeyma, A. & Khajehahmadi, S. (2015) The need for lateral piriform rim augmentation in patients with unilateral cleft lip/palate during alveolar cleft bone grafting. *Journal of Maxillofacial and Oral Surgery*, 14, 573–577.

Sasaki, A., Takeshita, S., Publico, A.S., Moss, M.L., Tanaka, E., Ishino, Y. et al. (2004) Finite element growth analysis for the craniofacial skeleton in patients with cleft lip and palate. *Medical Engineering and Physics*, 26, 109–118.

Urbanova, W., Brudnicki, A., Strydom, H., Bronkhorst, E.M., Katsaros, C. & Fudalej, P.S. (2013) Nasolabial aesthetics correlates poorly with skeletal symmetry in unilateral cleft lip and palate. *Journal of Plastic, Reconstructive and Aesthetic Surgery*, 66, e1–e7.

Wu, Y., Yang, Y., Chen, Y., Zhang, Y. & Wang, G. (2013) Measurement and evaluation of the alar base in unilateral secondary lip nasal deformities by three-dimensional computed tomography. *The Cleft Palate-Craniofacial Journal*, 50, 696–703.

Yang, L., Chen, Z. & Zhang, X. (2016) A cone-beam computed tomography evaluation of facial asymmetry in unilateral cleft lip and palate individuals. *Journal of Oral Science*, 58, 109–115.

Zhang, L., Lu, L.i., Li, Z.-J., Liu, Q., Yang, M.-L., Wang, X.-K. & et al. (2014) Anthropometric analysis of the maxillary bone and the alar base in unilateral cleft lip with secondary nasal deformity: classification of a piriform margin bony depression. *The Cleft Palate-Craniofacial Journal*, 51, 23–29.